

# Cubzac-les-Ponts Experimental Embankments on Soft Clay

## 1 Introduction

In the 1970's, a series of test embankments were constructed on soft clay at Cubzac-les-Ponts in France. These full-scale field tests were well-instrumented and are well-documented, and consequently provide an excellent case history. Two of the embankments are the subject of this article. Embankment A was built rapidly to failure to find the limiting height. Embankment B was later constructed to a lower height, to study the long term time-dependent consolidation of the soft foundation clay.

The purpose here is to demonstrate that GeoStudio has the features and capability to numerically simulate the deformations and stability of such embankments using a fully coupled effective stress/pore-pressure type of analysis.

There are many publications describing the tests, analyses and experiments carried out at Cubzac-les-Ponts. The data used to develop the analyses here was extracted from the books written by Wood (1990) and Leroueil et al. (1990). The rest of this article refers to these authors as the Researchers.

## 2 Site conditions

At the Cubzac-les-Ponts site, the upper two metres of the clay deposit is desiccated and over-consolidated due to the seasonal variations in the water table. For analysis purposes, the water table is taken to be at a depth of 1 m.

Below the upper desiccated crust there is a 7-m thick stratum of slightly over-consolidated soft clay. It is the performance of this soft clay that was at the heart of the field research.

Under the clay stratum there is coarse sand and gravel with a relatively high hydraulic conductivity. The static pressure head in the gravel is about 8 m, making the pore-pressure distribution more or less hydrostatic within the clay.

For modeling purposes, it is assumed that the pore-pressure in the underlying granular material will not change due to the embankment loading.

The original Researchers divided the soft clay into many different layers with slightly different properties. This refinement is not considered here. Both the upper crust and the underlying clay are simplified to be homogeneous isotropic soil units. This simplification does not seem to have a significant effect on the results, since the computed values are in reasonable agreement with values computed by others and with the field measurements.

## 3 Soil properties

### 3.1 Soft clay

The soft clay is characterized here using the Modified Cam-Clay (MCC) constitutive model available in SIGMA/W. It is an ideal constitutive model for this case, since it can account for pore-pressure changes arising from mean effective stress and deviatoric stress changes; an important feature in soft clay behavior.

The soil properties used to represent the stress-strain behavior and strength of the soft clay are shown in Table 1. The stiffness of the soil is controlled by the slopes of the isotropic normal compression line ( $\lambda$ ) and the unloading-reloading line ( $\kappa$ ).

In a SIGMA/W fully coupled consolidation analysis, it is necessary to define a volumetric water content (VWC) function and a hydraulic conductivity function, even though the soil is saturated and remains saturated during the embankment loading. The volumetric water content function is actually not used for saturated conditions, but is nonetheless required. An approximate estimated function is consequently adequate.

As with the VWC function, an approximate hydraulic conductivity function is adequate since only the saturated conductivity ( $K_{sat}$ ) is used in the analysis. A  $K_{sat}$  value of  $1.0 \times 10^{-4}$  m/day is used here for the clay (approximately  $8 \times 10^{-8}$  m/sec).

**Table 1 Soil properties for the soft clay**

Parameter	Value
Constitutive model	Modified Cam-Clay
Over-consolidation Ratio:	1.4
Poisson's Ratio ( $\nu$ ):	0.4
Lambda ( $\lambda$ ):	0.5
Kappa ( $\kappa$ ):	0.05
Initial Void Ratio:	2.25
Mu (M) ( $\phi' = 30^\circ$ ):	1.2
Unit Weight ( $\gamma$ ; kN / m <sup>3</sup> ):	15.0
$K_{sat}$ m/day	$1 \times 10^{-4}$

### 3.2 Desiccated crust

The properties used for the desiccated crust are listed in Table 2.

**Table 2 Soil properties for the desiccated crust**

Parameter	Value
Constitutive model	Linear-elastic
Young's Modulus $E$ (kPa):	3000
Poisson's Ratio ( $\nu$ ):	0.4
Unit Weight ( $\gamma$ ; kN / m <sup>3</sup> ):	16.5
Effective Friction Angle:	30°
Cohesion (kPa)	0
$K_{sat}$ m/day	$8 \times 10^{-4}$

A linear-elastic constitutive model is in part used for numerical stability reasons. Beyond the toe of the embankment, the insitu stresses are very small and the ground will tend to heave and go into tension. This can cause numerical convergence problems, since the elastic-plastic model, for example, cannot accommodate tension. Using a linear-elastic model avoids this problem. Any undesirable effect that this has on the results is considered minor, especially if the stiffness  $E$  is a low value.

The effective strength parameters are listed, since they are used in the stability analysis.

The water table is at mid-depth of the upper crust making the pore-pressure negative above the water table. To handle this correctly in a saturated-unsaturated coupled consolidation analysis, it is necessary to define a VWC function and a hydraulic conductivity function.

Figure 1 shows the volumetric water content function of the desiccated crust that was estimated from the built-in sample functions (KeyIn: Hydraulic Functions: Volumetric Water Content: Estimate: Estimation Method: Sample Functions: Silty Clay). The function was generated using a saturated volumetric water content of 0.3 with all other parameters at the default values.

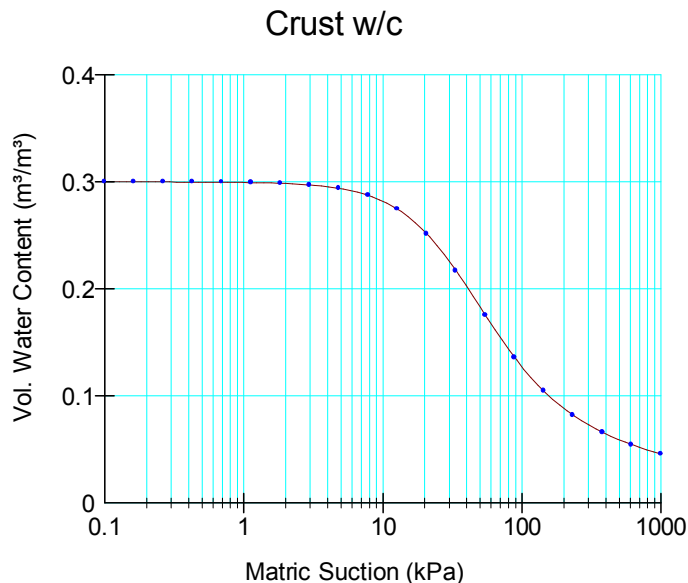


**Figure 1 Volumetric water content function for the crust**

The air entry value for this VWC function is around 10 kPa suction. This implies that the soil above the water table is more or less saturated, but the pore-pressure is negative. This is referred to as a tension-saturated zone. It means that the pore-pressure will become positive quickly as the embankment load is applied.

Figure 2 shows the hydraulic conductivity function used for the desiccated crust. It was estimated from the volumetric water content function using the van Genuchten technique (KeyIn: Hydraulic Functions: Hydraulic Conductivity: Estimate: Estimation Method: van Genuchten). The function was generated using a saturated hydraulic conductivity of  $8.0 \times 10^{-4}$  m/day (approximately  $1 \times 10^{-8}$  m/sec) and a residual volumetric water content of 0.04. All other parameters were left at the default values.

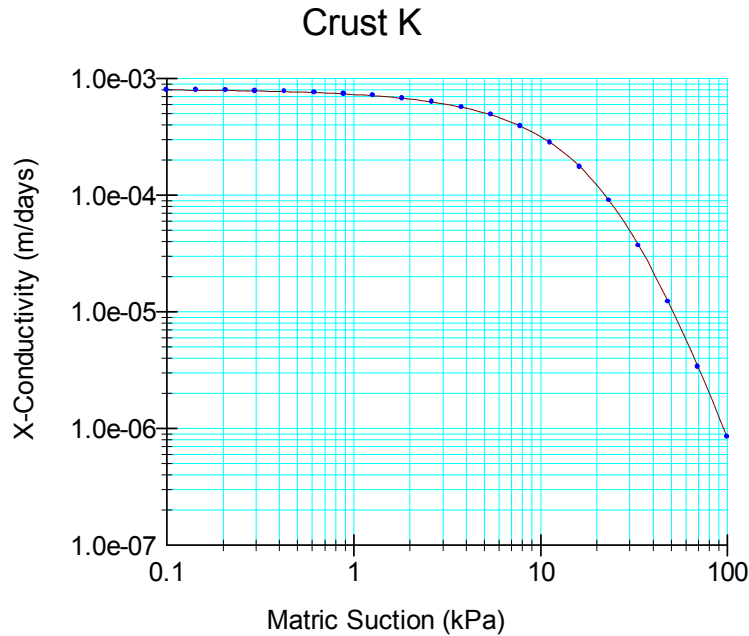


Figure 2 Hydraulic conductivity function for the desiccated crust

### 3.3 Embankment fill

The embankment fill is modeled using a simple linear elastic model with total stress parameters. The material used for the embankment construction is coarse sand and gravel. The pore-pressure for such a material can be ignored in the numerical model. This is achieved in SIGMA/W by assigning the fill Total Stress material properties. Hydraulics properties are consequently not required for the fill. All other relevant material properties are listed Table 3.

Table 3 Soil properties for the embankment fill

Parameter	Value
Model:	Linear-Elastic
Young's Modulus $E$ (kPa):	3000
Poisson's Ratio ( $\nu$ ):	0.4
Unit Weight ( $\gamma$ ; kN / m <sup>3</sup> ):	21.0
Effective Friction Angle:	35°
Cohesion (kPa)	0 kPa

## 4 Embankment A

As noted in the introduction, Embankment A was constructed rapidly to determine the height or conditions at which failure would occur. The cross-section used to model this part of the field experiment

is shown in Figure 3. First, a 1.5 m lift was placed over a wide area. Next three 1 m lifts were placed to one side to ensure that the failure would be to the right.

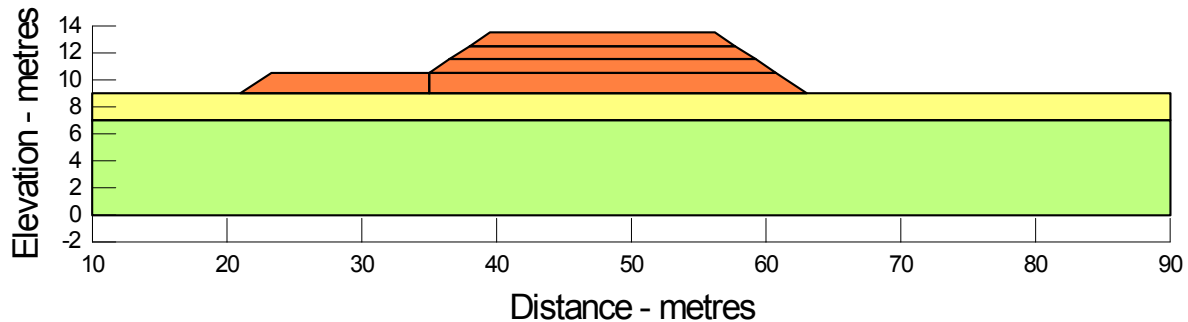


**Figure 3 Embankment A used to determine failure conditions**

The fill was placed over a period of eight days. On Day 1, the fill reached 1.5 m. Additional 1 m lifts were placed on Day 5, Day 7 and Day 8. This sequence is detailed in the SIGMA/W time stepping specification.

The analysis tree is given in Figure 4. The first analysis establishes the insitu stress condition before the fill placement starts. Lift 1 is placed on Day 1, but the analysis covers 4 days. Lift 2 has a time-duration of 2 days. Lifts 3 and 4 each have a time-duration of 1 day. The fill placement took place over 8 days when the failure started. The last analysis is a slope stability analysis used to compute the factor of safety when the failure started.

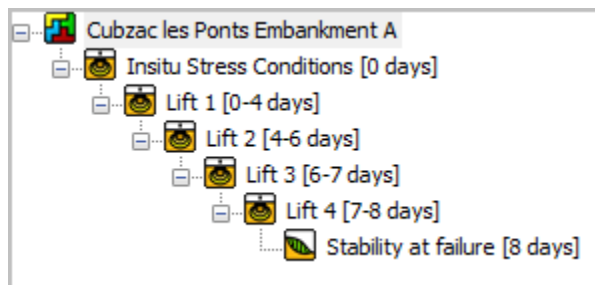


**Figure 4 Embankment A analysis tree**

#### 4.1 Starting insitu conditions

It is mandatory to establish the starting insitu stress conditions whenever a nonlinear constitutive model is to be used. Since we are using the MCC model, it is essential to first establish the starting ground conditions. In SIGMA/W this can be done with the Insitu type of analysis.

The  $K_0$  condition in SIGMA/W is specified through Poisson's ratio  $\nu$ . Recall that  $K_0$  in a 2D analysis is equivalent to  $\nu/(1-\nu)$ . The specified  $\nu = 0.4$  in this case represents a  $K_0$  of 0.667. The resulting total and effective stress profiles are shown in Figure 5 and Figure 6. The ratio of the effective stresses at the base of the problem, for example, is close to 0.667, confirming that the computed insitu stresses correspond with the anticipated values.

The specified unit weights are used to apply the self weight of the material.

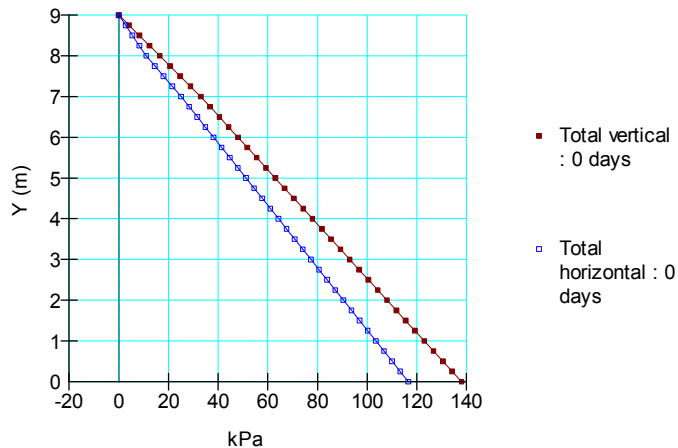


Figure 5 Total vertical and horizontal insitu stress profiles

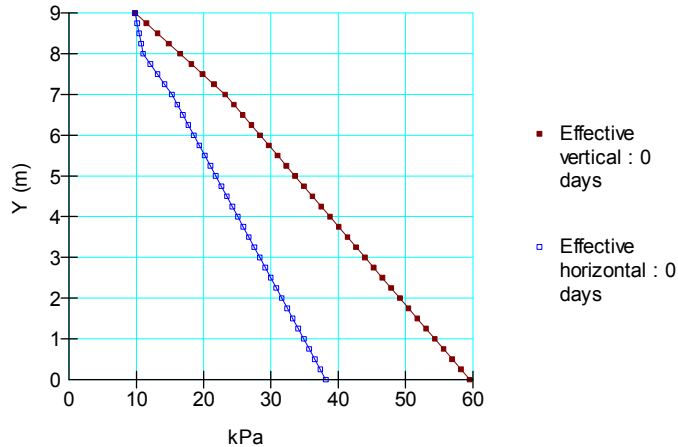


Figure 6 Effective vertical and horizontal insitu stress profiles

## 4.2 Hydraulic boundary conditions

At the start of the analysis, it is not known how much the water table will rise due to the loading. The possibility of the water table coming up to contact the base of the fill can be covered with the specification of a potential seepage face review boundary. The effect of this is that if the computed total head is greater than the elevation, the boundary condition is converted to a Head-type, with the action equal to the y-coordinate, which represents zero pore-pressure.

Earlier it was noted that the water pressure in the underlying gravel will be assumed to not change as a result of the loading. This condition can be maintained by specifying a Head equal to 8 m along the base of the problem.

## 4.3 Rise in water table

When the first lift is placed, the water table rises slightly, as shown in Figure 7. By the end of the fill placement, the water table (zero pore-pressure line) has reached the base of the fill, as shown in Figure 8.

By treating the fill as a Total Stress material which leaves the pore-pressure undefined, the assumption is that any water squeezed out of the foundation clay will have the opportunity to disappear laterally somehow.

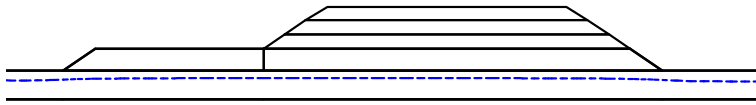


**Figure 7 Position of the water table on Day 1 after first lift**

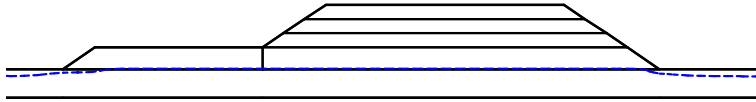


**Figure 8 Position of water table after last lift**

Figure 9 demonstrates how the pore-pressure increases with time at a point under the center of the fill at the clay-fill contact level. Once the positive pore-pressure reaches the contact level where the boundary condition is specified as potential seepage face, the pore-pressure remains at zero (Day 6).

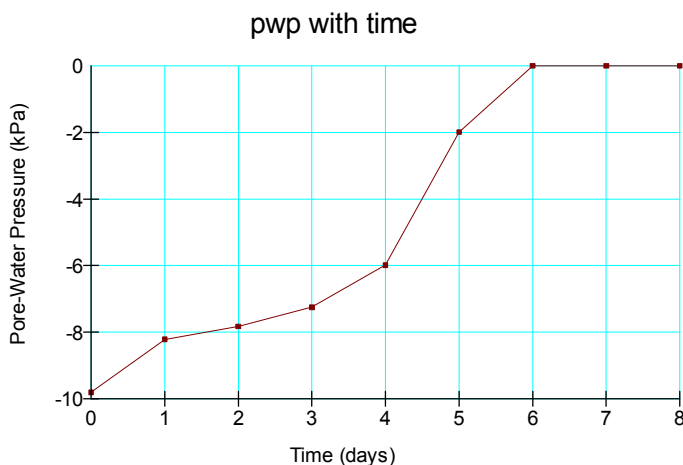


**Figure 9 Pore pressure rise in crust with time during fill placement**

This behavior is consistent with what one would intuitively expect, and demonstrates how SIGMA/W can correctly model saturated-unsaturated consolidation.

#### 4.4 Ground surface settlements

Figure 10 shows the settlement profiles at the four loading stages. The numbers beside the series symbols are days from start of construction. The maximum computed settlement is approximately 0.16 m (16 cm). The maximum measured settlement in the field was slightly greater than 20 cm. The simulated total settlement could easily be improved by better accommodating the spatial variability of the material parameters; however, the important point is that the computed and measured patterns of behavior are very similar. The agreement between measured and computed settlements is actually rather remarkable, in light of the complex spatial variations of material properties. Furthermore, the end of construction

settlement reading was recorded when the foundation materials were in a failed state and therefore possibly accelerating.

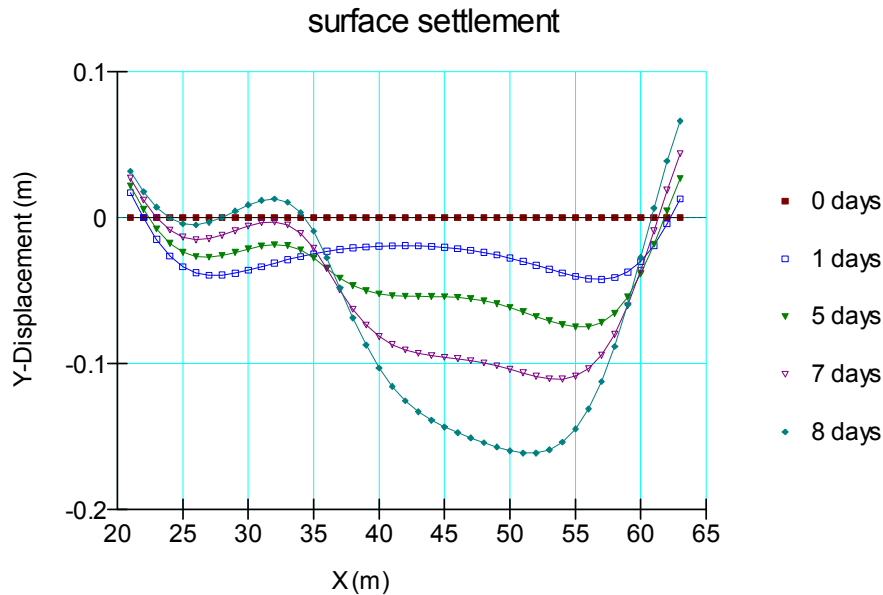


**Figure 10 Settlement profiles under the embankment at the four loading stages**

Of some interest is the unsymmetrical shape in the maximum settlement along the surface profile. The maximum tends to the right side, which reflects the movement in the direction of the failure.

Figure 11 shows the excess pore-pressures in the foundation under the center of the embankment. The maximum excess pore pressure is about 90 kPa upon completion of the fill placement, which is nearly identical to the values generated by finite element analyses of other researchers (generally between 80 and 100 kPa). The predictions at other stages (e.g. fill height of 3.5 m) are also in agreement with the work of other researchers. In actuality, the measured excess pore-pressures were less than the simulated values at all stages of the analysis. The soft clay pore pressure did not respond at 100% of the applied total stress. This response has been attributed to the water having a finite compressibility due to the presence of gas bubbles.

SIGMA/W has a parameter called a *Load Response Ratio*. This parameter can be used simulate a pore-pressure response of less than 100%. In this case, the parameter is 1.0, meaning the conventional full response assuming the water is incompressible. While this somewhat overestimates the measured pore-pressures, it gives a more acceptable response in the distribution.

The Load Response Ratio must be used with some caution, since it is affected by the Poisson's ratio.

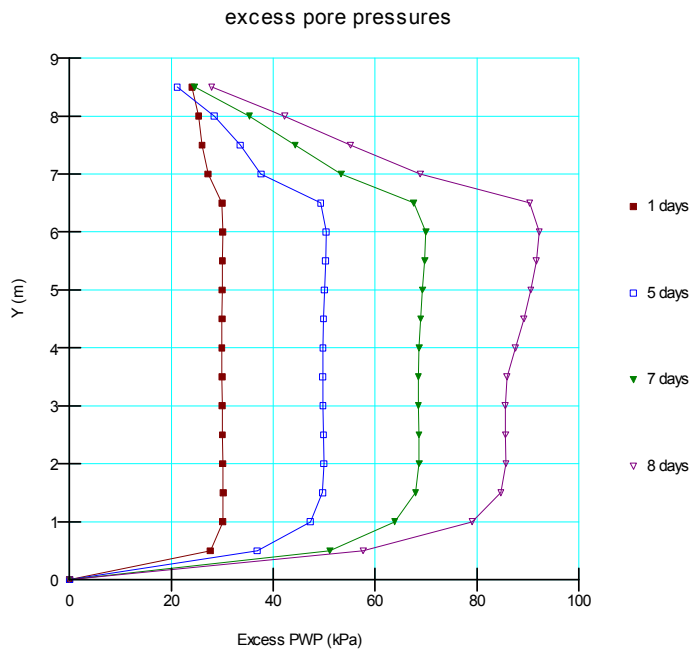


Figure 11 Excess pore-water pressure under the center of the embankment

#### 4.5 Stability calculations at failure

After reaching a fill height of 4.5 m, the embankment failed. By definition, the factor of safety fell to 1.0. Interestingly, when the SIGMA/W computed stresses and pore-pressures are used in a SLOPE/W stability analysis, the minimum factor of safety is right around 1.0, as illustrated in Figure 12.

This close agreement between the computed stability and the actual failure is notable.

The red band in Figure 12 shows a zone of possible slips with safety factors between 1.029 and 1.079. The white line within the band is the slip surface with a factor of safety of 1.029.

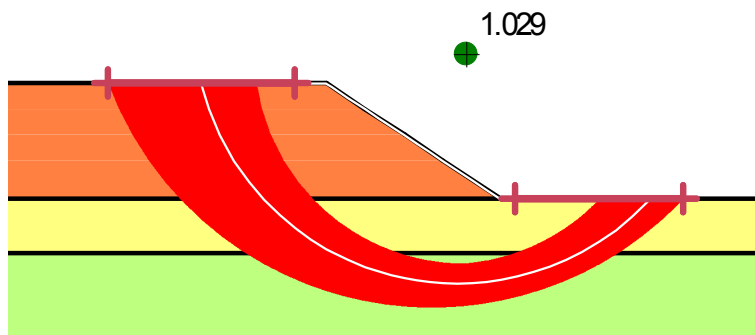


Figure 12 Computed stability safety factor at the time of failure

## 5 Embankment B

Embankment B (Figure 13) was constructed to a height of 2.4 m over a period of six days. For this analysis, the fill placement is simulated with six even lifts, one lift per day. Settlements, pore-pressures and lateral deformations were then monitored over the next five years.

The material properties for Embankment B are the same as for Embankment A.

The analysis tree for Embankment B is shown in Figure 14.

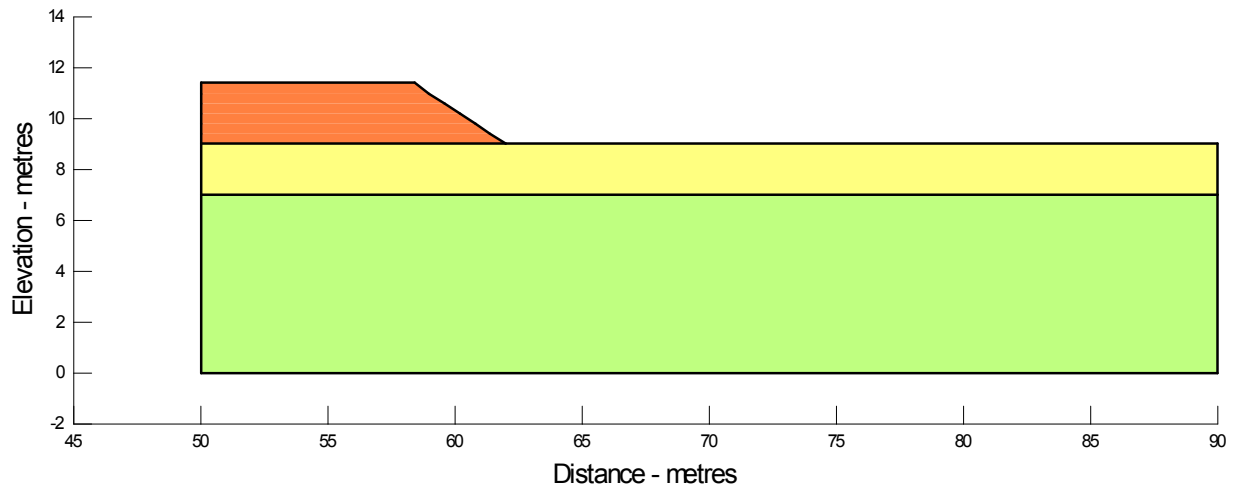


Figure 13 Embankment B configuration

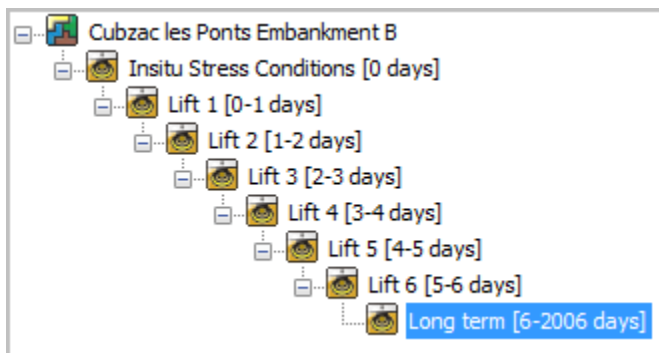
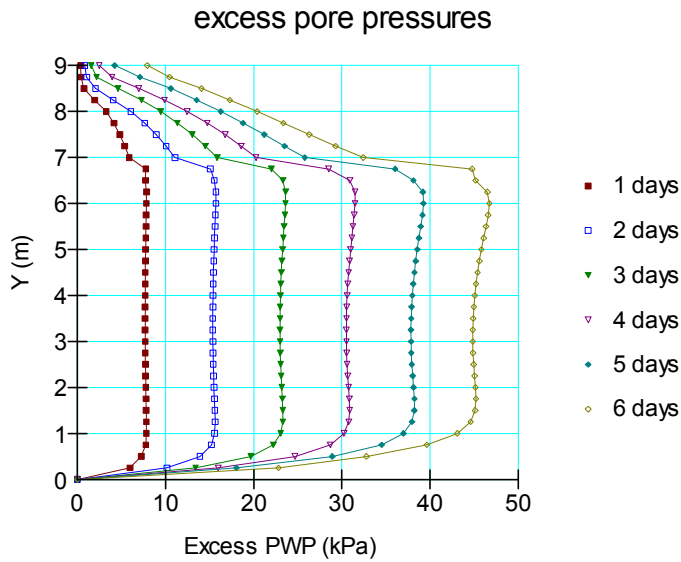


Figure 14 Analysis tree for Embankment B

### 5.1 Excess pore-pressures

The build-up of excess pore-pressures due to the six days of embankment construction is shown in Figure 15. The patterns of the field measured excess pore-pressure profiles were considerably more variable (not as uniform) than those shown in Figure 15. The peak measured pore-pressures, however, were in the range of 40 to 50 kPa, the same as the computed values at the end of the fill placement.



**Figure 15 Buildup of excess pore-pressures during fill placement**

## 5.2 Pore-Pressure Dissipation

During the long-term monitoring, the excess pore-pressure dissipated, as shown Figure 16. After 2006 days (5.5 years), the computed excess pore-pressure has diminished to a maximum of about 10 kPa. This dissipation is somewhat greater than what happened in the field. The maximum measured values at the end of the same time period, however, were more like 25 kPa.

The simulation could perhaps be improved by incorporating more of the actual spatial variations in the material properties. While the actual measured and computed values vary somewhat, the profile patterns and trends are remarkably similar. In this sense, the numerical model represents the field performance very well.

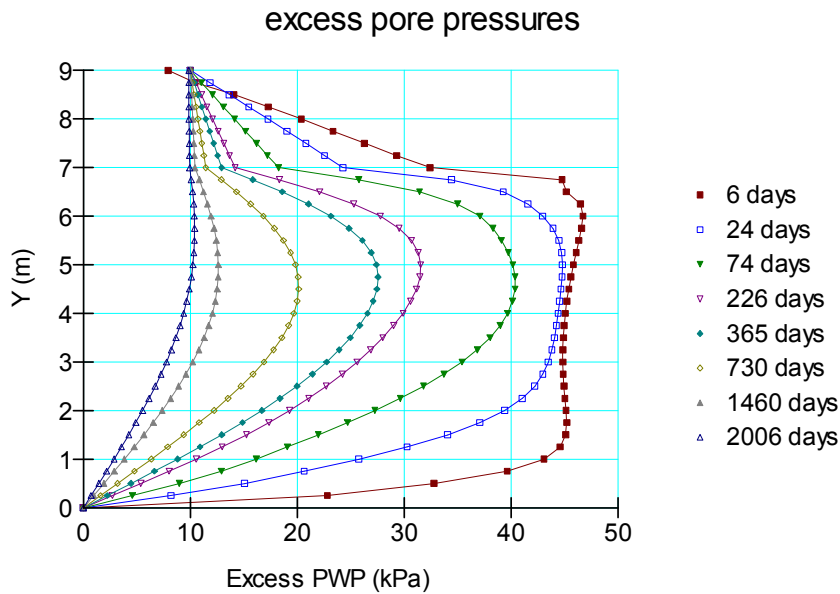


**Figure 16 Long-term dissipation of excess pore-pressures**

A small amount of excess pore-pressure (about 10 kPa) remains after five years. Dissipating this excess pore-pressure takes a very long time. After 15 years, for example, the excess pore-pressure may have reduced to 5 kPa. Eventually, however, the pore-pressure will return to the starting conditions, all else being the same.

### 5.3 Long-Term Settlement

Figure 17 shows the long-term consolidation settlement profiles under the embankment. The maximum computed settlement after five years is around 0.4 m (400 mm). This value is about half the actual measured maximum settlement, which was around 0.8 m.

Once again, attempts could be made to alter the material properties to try to obtain a closer match. However, that is beyond the objective of this illustrative example.

Even a difference of 400 mm between the computed and measured settlement is reasonable agreement, when considering the scale of the embankment, the natural material variability and the very long monitoring period.

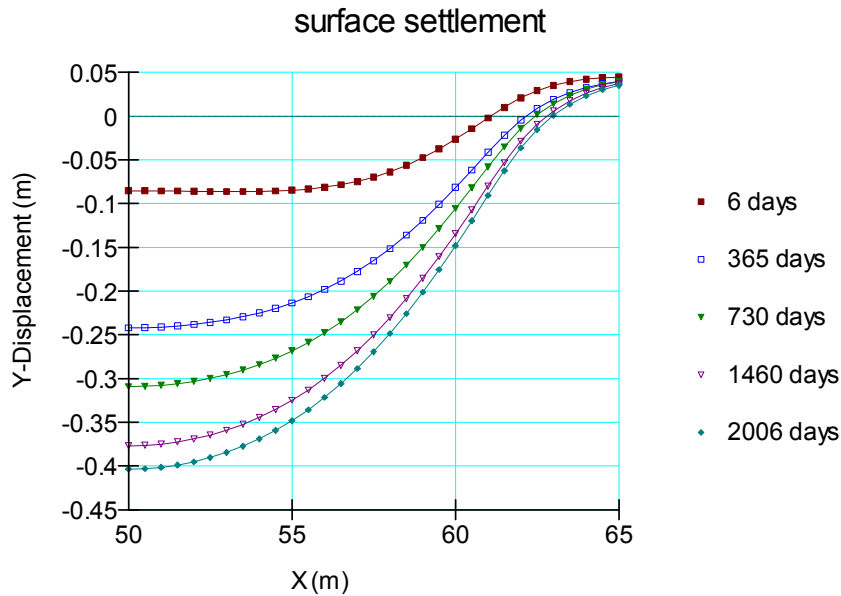


Figure 17 Long-term settlement of the original ground surface

#### 5.4 Horizontal Movement

The computed horizontal movements at the toe of Embankment B are presented in Figure 18. At the end of construction on Day 6, the maximum computed lateral movement is around 100 mm. During the long consolidation period, the computed results show only an additional 15 mm of lateral movement. up to 115 mm.

The field inclinometer profiles are shown in Figure 19. At the end of construction, the lateral movement was only about 25 mm, but then slowly increased during the consolidation to about 130 mm.

The measured and computed lateral deflections at the end of the fill placement are compared in Figure 20. The same comparison after five years is shown in Figure 21. As is evident from these two figures, the agreement between measured and computed deflections after 5 years is reasonably good. However, the comparison is rather poor at the end of the fill placement. The reason for this difference is not clear, as there does not appear to be any intuitive logical reason for this.

Of greater significance than the magnitude of the lateral deflections is the position of the maximum displacement that occurs in the soft clay just below the desiccated crust. This is also the zone where the failure slip surface was in Embankment A.

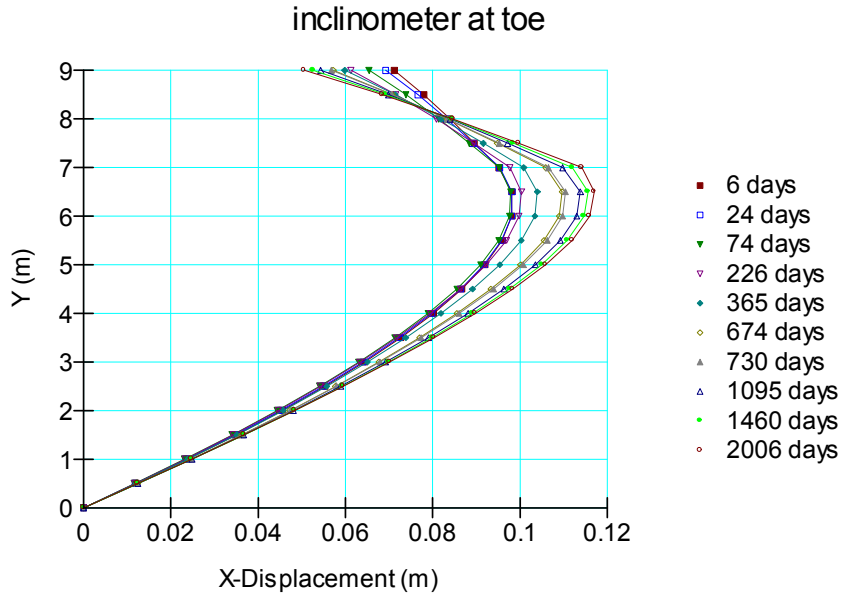


Figure 18 Computed lateral deflections at the toe of the embankment

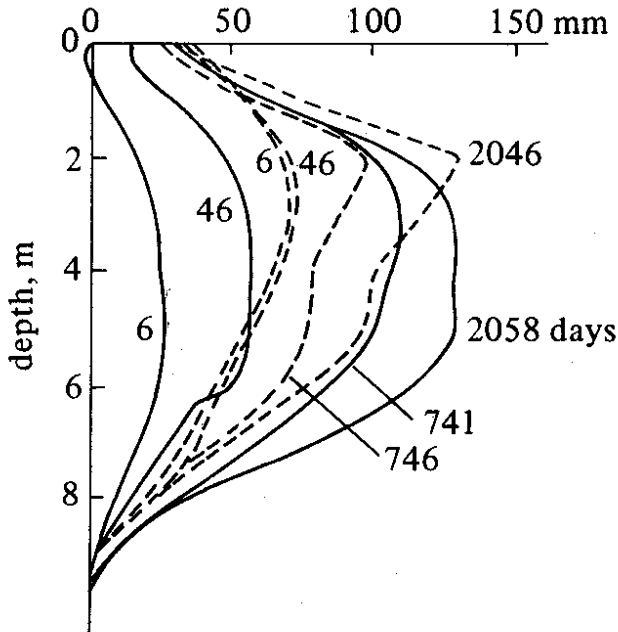


Figure 19 Field inclinometer profiles (solid lines) at the toe of Embankment B (Wood,1990 p. 406)

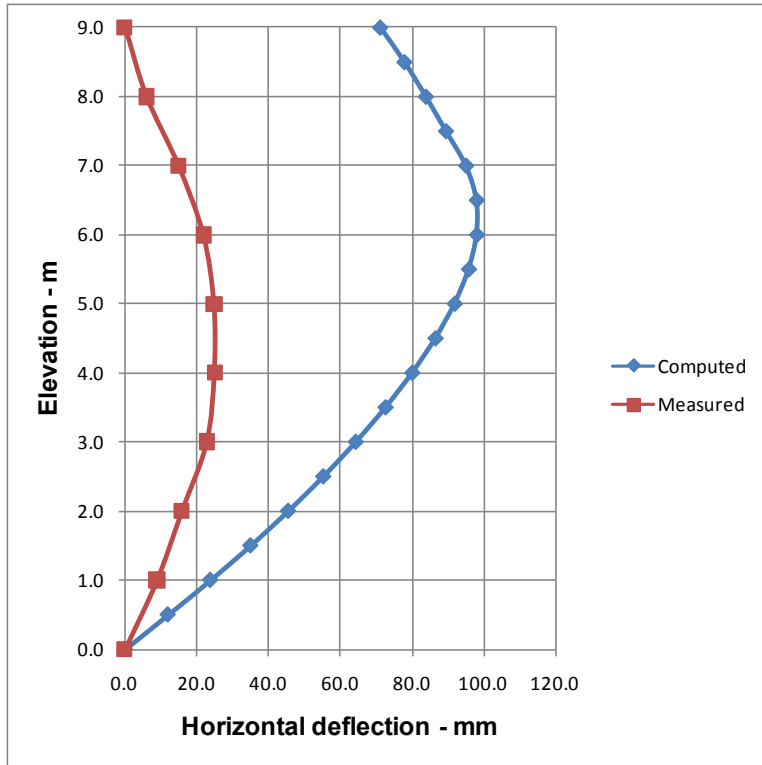


Figure 20 Comparison of horizontal deflections at the end of fill placement

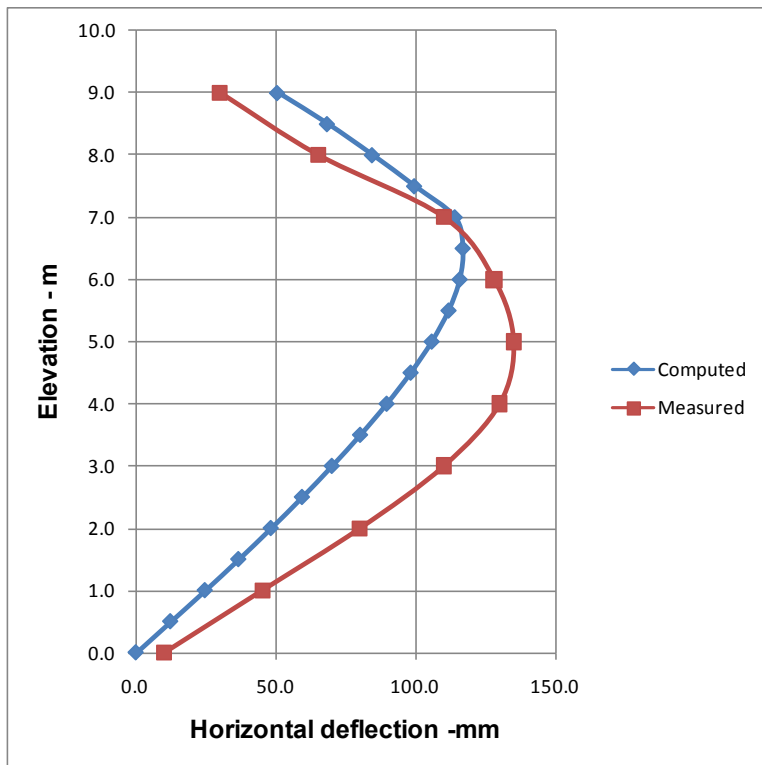


Figure 21 Comparison of horizontal deflections after 5 years

## **6 Concluding remarks**

There is much more that could be done in analyzing the deformation response of these two embankments. A great amount of field and laboratory measurements are available. This data could be used to refine the analysis and more closely simulate the observed behavior. For example, the clay could be divided into various layers with each layer having slightly different properties. The soft clay immediately under the desiccated crust has a much higher organic content than the underlying soils. The higher organic content is normally associated with an increase in compressibility and hydraulic conductivity. In fact, the slope of the isotropic compression line ( $\lambda$ ) was measured to be around 0.7 and 1.0 between depths of 2 and 4 m. Incidentally, this depth range corresponds to the location of the uniform lateral displacements and large settlements.

Of significance is that reasonable agreement between the measured and computed values for key deformation behaviors (that is, settlement, pore- pressure, and lateral deformations) can be obtained with a simple set of material properties and boundary conditions. Furthermore, and perhaps more importantly, the occurrence of failure at the end of construction was appropriately predicted for Embankment A.

Obtaining reasonable results from a simplified approach of a real field case shows that it is not always necessary to try and duplicate all of the field intricacies. Useful and meaningful results can be obtained from a simplified numerical model of the actual field conditions. Whether this is true in all cases must be judged in light of the objective of the analysis.

Most important in this case is the demonstration that GeoStudio has all the features and capabilities for analyzing all aspects of a real field case such as the experimental test embankments at Cubzac-les-Ponts.

## **7 References**

- Leroueil, S., Magnan, J.P., and Tavenas, F. 1990. Embankments on Soft Clay. Ellis Horwood, New York.
- Wood, D.M. 1990. Soil Behaviour and Critical State Soil Mechanics. Cambridge University Press, Cambridge.